Formation of New η^5-Rhodium(III) Complexes from η^5-Rh(I) Rhodacarborane-Containing Charge-Compensated Ligands

R. Núñez,† O. Tutusaus,† F. Teixidor,*,† C. Viñas,† R. Sillanpää,‡ and R. Kivekäs§

Institut de Ciència de Materials, CSIC, Campus U.A.B., 08193 Bellaterra, Spain, Department of Chemistry, University of Jyväskylä, FIN-40351, Jyväskylä, Finland, and Department of Chemistry, P.O. Box 55, University of Helsinki, FIN-00014, Finland

Received October 14, 2003

A series of new Rh(I) half-sandwich complexes of formula [3,3-$(PPh_3)_2$-8-L-*closo*-3,1,2-$RhC_2B_9H_{10}$)] (L = SMe_2 (**2a**), SEt_2 (**2b**), $S(CH_2)_4$ (**2c**), SEtPh (**2d**)) and [1-Me-3,3-$(PPh_3)_2$-8-L-*closo*-3,1,2-$RhC_2B_9H_9$)] (L = SMe_2 (**2e**), SEt_2 (**2f**)) have been prepared by reaction of the respective monoanionic charge-compensated ligands $[10\text{-L-}nido\text{-}7,8\text{-}C_2B_9H_{10}]^-$ and $[7\text{-Me-}10\text{-L-}7,8\text{-}C_2B_9H_9]^-$ with $[RhCl(PPh_3)_3]$. Complex [3,3-(cod)-8-SMe_2-*closo*-3,1,2-$RhC_2B_9H_{10}$] (**3**) has also been prepared by reaction of K[10-SMe_2-*nido*-7,8-$C_2B_9H_{10}$] with $[RhCl(cod)]_2$. Rh(I) complexes **2a**−**d** may be easily oxidized to the corresponding Rh(III) complexes **4a**−**d** under N_2 atmosphere in some halogenated solvents such as CCl_4 and $CHCl_3$. The complexes have been fully characterized by IR and NMR spectroscopy, and the crystal structures of **2a**, **3**, and **4a** have been elucidated by single-crystal X-ray diffraction analysis. An EPR spectrum analysis clearly evidences the formation of free radicals as intermediates in the evolution of **2a**−**d** to **4a**−**d** complexes. The capacity to stabilize both Rh(I) and Rh(III) oxidation states by the $[10\text{-}SMe_2\text{-}nido\text{-}7,8\text{-}C_2B_9H_{10}]^-$ system may be attributed to its donor capacity together with the presence of labile ligands in the molecule.

Introduction

To date, a large number of metallacarboranes of the type *closo*-MC_2B_9 have been prepared and structurally characterized using the $[C_2B_9H_{11}]^{2-}$ dianionic dicarbollide ligand.[1] Also a few transition metal complexes[2−5] with monoanionic charge-compensated ligands of the type $[LC_2B_9H_{10}]^-$ (L = pyridine, THF, SR_2, PPh_3, OEt_2, NR_3, etc.) have been reported.[6] In general, all these complexes have been designed to establish detailed comparisons with their analogous cyclopentadienyl-metal complexes.[7] The main difference between both types of dicarbollide ligands is the charge. In this respect, it is generally accepted that the dianionic $[C_2B_9H_{11}]^{2-}$ cluster stabilizes higher oxidation states than the monoanionic $[LC_2B_9H_{10}]^-$ ligands. Among the latter, the ligand

† Institut de Ciència de Materials, CSIC.
‡ University of Jyväskylä.
§ University of Helsinki.

(1) (a) *Contemporary Boron Chemistry*; Davidson, M., Hughes, A. K., Marder, T. B., Wade, K., Eds.; Royal Society of Chemistry: Cambridge, U.K., 2000. (b) *Advances in Boron Chemistry*; Siebert, W. E., Ed.; Royal Society of Chemistry: Cambridge, U.K., 1997. (c) *The Borane-Carborane-Carbocatiom Continuum*; Casanova, J., Ed.; Wiley-Interscience: New York, 1998. (d) *Comprehensive Organometallic Chemistry II*; Abel, E. W., Stone, F. G. A., Wilkinson, G., Eds.; Pergamon Press: Oxford, England, 1995; Vol. 1. (e) *Boron Chemistry at the Beginning of the 21st Century*; Bubnov, Yu. N., Ed.; Editorial URSS: Moscow, 2003.

(2) (a) Hawthorne, M. F.; Warren, L. F., Jr.; Callahan, K. P.; Travers, N. F. *J. Am. Chem. Soc.* **1971**, *93*, 2407. (b) Plesek, J.; Janousek, Z.; Hermanek, S. *Collect. Czech. Chem. Commun.* **1978**, *43*, 2862. (c) Wong, E. H. S.; Hawthorne, M. F. *Inorg. Chem.* **1978**, *17*, 2863. (d) Colquhoun, H. M.; Greenhough, T. J.; Wallbridge, M. G. H. *J. Chem. Soc., Dalton Trans.* **1979**, 619. (e) Teller, R. G.; Wilczynski, J. J.; Hawthorne, M. F. *J. Chem. Soc., Chem. Commun.* **1979**, 472. (f) Marder, T. B.; Baker, R. T.; Long, J. A.; Doi, J. A.; Hawthorne, M. F. *J. Am. Chem. Soc.* **1981**, *103*, 2988. (g) King, R. E., III; Miller, S. B.; Knobler, C. B.; Hawthorne, M. F. *Inorg. Chem.* **1983**, *22*, 3548. (h) Kang, H. C.; Do, Y.; Knobler, C. B.; Hawthorne, M. F. *J. Am. Chem. Soc.* **1987**, *109*, 6530. (i) Kang, H. C.; Do, Y.; Knobler, C. B.; Hawthorne, M. F. *Inorg. Chem.* **1988**, *27*, 1716.

(3) (a) Hamilton, E. J. M.; Welch, A. J. *Acta Crystallogr.* **1990**, *C46*, 1228. (b) Cowie, J.; Hamilton, E. J. M.; Laurie, J. C. V.; Welch, A. J. *J. Organomet. Chem.* **1990**, *394*, 1. (c) Hamilton, E. J. M.; Welch, A. J. *Polyhedron* **1991**, *10*, 471. (d) Douek, N. L.; Welch, A. J. *J. Chem. Soc, Dalton Trans.* **1993**, 1917. (e) Rosair, G. M.; Welch, A. J.; Weller, A. S.; Zahn, S. K. *J. Organomet. Chem.* **1997**, *536*−*537*, 299. (f) Dunn, S.; Rosair, G. M.; Weller, A. S.; Welch, A. J. *Chem. Commun.* **1998**, 1065. (g) Rosair, G. M.; Welch, A. J.; Weller, A. S. *Organometallics* **1998**, *17*, 3227, (h) Boyd, A. S. F.; Rosair, G. M.; Tiarks, F. B. H.; Weller, A. S.; Zahn, S. K.; Welch, A. J. *Polyhedron* **1998**, *17*, 2627. (i) Johansen, K.; Rosair, G. M.; Weller, A. S.; Welch, A. J. *Acta Crystallogr.* **1998**, *C 54*, 214.

(4) (a) Yan, Y-.K.; Mingos, D. M. P.; Müller, T. E.; Williams, M.; Kurmoo, J. *J. Chem. Soc., Dalton Trans.* **1994**, 1735. (b) Yan, Y-.K.; Mingos, D. M. P.; Müler, T. E.; Williams, M.; Kurmoo, J. *J. Chem. Soc., Dalton Trans.* **1995**, 2509. (c) Kudinov, A. R.; Meshcheryakov, V. I.; Petrovskii, P. V.; Rybinskaya, M. I. *Izv. Akad. Nauk. Ser. Khim.* **1999** 177 [*Russ. Chem. Bull.* **1999**, 48, 176 (Engl. Transl.)]. (d) Kudinov, A. R.; Petrovskii, P. V.; Meshcheryakov, V. I.; Rybinskaya, M. I. *Izv. Akad. Nauk. Ser. Khim.* **1999**, 1368 [*Russ. Chem. Bull.* **1999**, 48, 1356 (Engl. Transl.)].

(5) (a) Kudinov, A. R.; Meshcheryakov, V. I.; Petrovskii, P. V.; Rybinskaya, M. I. *Izv. Akad. Nauk. Ser. Khim.* **1999**, 1817 [*Russ. Chem. Bull.* **1999**, *48*, 1794 (Engl. Transl.)]. (b) Kudinov, A. R.; Perekalin, D. S.; Petrovskii, P. V.; Lyssenko, K. A.; Grintselev-Knyazev, G. V.; Starikova, Z. A. *J. Organomet. Chem.* **2002**, *657*, 115.

(6) (a) Tebbe, F. N.; Garret, P. M.; Hawthorne, M. F. *J. Am. Chem. Soc.* **1968**, *90*, 869. (b) Plešek, J.; Zbyněk, J.; Heřmánek, S. *Collect. Czech. Chem. Commun.* **1978**, *43*, 2862. (c) Plešek, J.; Janousek, Z.; Heřmánek, S. *Inorg. Chem.* **1983**, *22*, 239. (d) Kang, H. C.; Lee, S. S.; Knobler, C. B.; Hawthorne, M. F. *Inorg. Chem.* **1991**, *30*, 2024. (e) Plešek, J.; Jelínek, T.; Mares, F.; Heřmánek, S. *Collect. Czech. Chem. Commun.* **1993**, *58*, 1534. (f) Rosair, G. M.; Welch, A. J.; Weller, A. S.; Zahn, S. K. *J. Organomet. Chem.* **1997**, *536*, 299. (g) Dunn, S.; Garrioch, R. M.; Rosair, G. M.; Smith, L.; Welch A. J. *Collect. Czech. Chem. Commun.* **1999**, *64*, 1013. (h) Tutusaus, O.; Teixidor, F.; Núñez, R.; Viñas, C.; Kivekäs, R.; Sillanpää, R. *J. Organomet. Chem.* **2002**, *657*, 247.

(7) *Comprehensive Organometallic Chemistry*; Wilkinson, G., Stone, F. G. A., Abel, E. W., Eds.; Pergamon: Oxford, 1981.

10.1021/om030635h CCC: $27.50
Publication on Web 04/03/2004

Scheme 1. Formation of $[3,3\text{-}(PPh_3)_2\text{-}8\text{-}L\text{-}closo\text{-}3,1,2\text{-}RhC_2B_9H_{10}]$ or $[1\text{-}Me\text{-}3,3\text{-}(PPh_3)_2\text{-}8\text{-}L\text{-}closo\text{-}3,1,2\text{-}RhC_2B_9H_9]$

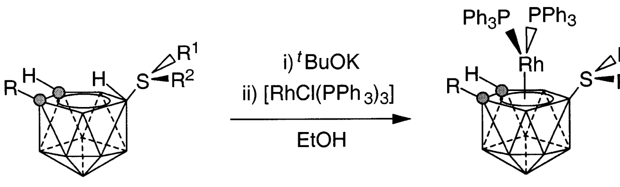

1a-f **2a-f**

a: R=H, SR[1]R[2] = SMe₂
b: R=H, SR[1]R[2] = SEt₂
c: R=H, SR[1]R[2] = tht
d: R=H, SR[1]R[2] = SEtPh
e: R=Me, SR[1]R[2] = SMe₂
f : R=Me, SR[1]R[2] = SEt₂

$[9\text{-}SMe_2\text{-}nido\text{-}7,8\text{-}C_2B_9H_{10}]^-$ is the most convenient to synthesize; hence it has been the most widely studied.[6c] We have recently reported[6h] a series of charge-compensated monoanionic ligands with general formula $[10\text{-}R_2S\text{-}nido\text{-}7,8\text{-}C_2B_9H_{10}]^-$, which seem to be capable of stabilizing two consecutive oxidation states in a metal.[8] This can be very relevant in different steps of a catalytic process. In fact, ruthenium complexes $[3\text{-}H\text{-}3,3\text{-}PPh_3\text{-}8\text{-}L\text{-}closo\text{-}3,1,2\text{-}RuC_2B_9H_{10}]$ of these ligands, analogous to $[RuClCp'(PR_3)_2]$ (Cp′= Cp, substituted Cp), have been proven to be very active in cyclopropanation, radical polymerization, and Kharasch addition catalytic reactions.[8,9]

On the other hand, half-sandwich rhodium complexes containing a Cp′ ligand, such as $[RhCp'Cl_2(PPh_3)]$ and $[RhCp'(PPh_3)_2]$, are efficient catalysts for olefin hydrogenation.[10] Nevertheless, until now, few Rh(I)[2e,f,3d,e] and Rh(III)[3h,5] complexes with dicarbollide charge-compensated ligands have been described.

In this paper we report on the synthesis and characterization of a new series of half-sandwich rhodium complexes analogous to $[RhCp'(PPh_3)_2]$ and $[RhCp'Cl_2(PPh_3)]$, respectively, in which the Cp′ has been replaced by the dicarbollide charge-compensated ligand $[10\text{-}L\text{-}nido\text{-}7,8\text{-}C_2B_9H_{10}]^-$. The donating capacity of the ligand makes it able to stabilize both Rh(I) and Rh(III) complexes, metal ions in oxidation states separated by two units.

Results and Discussion

Synthesis and chaRacterization of $[3,3\text{-}(PPh_3)_2\text{-}8\text{-}L\text{-}closo\text{-}3,1,2\text{-}RhC_2B_9H_{10}]$ and $[1\text{-}Me\text{-}3,3\text{-}(PPh_3)_2\text{-}8\text{-}L\text{-}closo\text{-}3,1,2\text{-}RhC_2B_9H_9]$ (L = SMe_2, SEt_2, $S(CH_2)_4$, SEtPh). The neutral charge-compensated *nido*-carboranes of general formula $7\text{-}R\text{-}10\text{-}L\text{-}nido\text{-}7,8\text{-}C_2B_9H_{10}$ (R = H; L = SMe_2 (**1a**), SEt_2 (**1b**), $S(CH_2)_4$ (**1c**), SEtPh (**1d**), and R = Me; L = SMe_2 (**1e**), SEt_2 (**1f**)) react quantitatively with K[*t*-BuO] in degassed ethanol to form the corresponding anionic species. The reaction of any of the anionic ligands with $[RhCl(PPh_3)_3]$, in a 1:1 ratio, afforded dark yellow solids formulated as $[1\text{-}R\text{-}3,3\text{-}(PPh_3)_2\text{-}8\text{-}L\text{-}closo\text{-}3,1,2\text{-}RhC_2B_9H_9)]$ (R = H; L = SMe_2 (**2a**), SEt_2 (**2b**), $S(CH_2)_4$ (**2c**), SEtPh (**2d**) and R = Me; L = SMe_2 (**2e**), SEt_2 (**2f**)). The reaction is shown in Scheme 1.

The ^1H NMR, ^{31}P NMR, and ^{11}B NMR spectra of complexes **2a**−**d** are consistent with a C_s symmetry molecule, while complexes **2e** and **2f** exhibit a C_1 symmetry. In the ^1H NMR spectra, the two distinct methylene protons in complexes **2b**, **2c**, and **2f** exhibit an ABC_3 spin system with $^1J_{HaHb}$ = 13.4 Hz and $^3J_{Ha,bHc}$ = 7.4 Hz (Table 1). The aromatic region shows resonances centered at 7.45 ppm, fitting six phenyl rings for all complexes, except for **2d**, which fits seven. The $^{11}B\{^1H\}$ NMR resonances appear between 2.0 and −23.0 ppm, in the region usual for *closo*-complexes. All signals are split into doublets (^1J(B,H) = 129−145 Hz) except the lowest field resonance assigned to the sulfur bearing a B(8) vertex, when ^{11}B NMR spectra were recorded. The $^{31}P\{^1H\}$ NMR spectra of compounds **2a**−**d** display one doublet with ^1J(Rh,P) = 192 Hz (Table 2). Two doublets of doublets are observed for complexes **2e** and **2f** with ^1J(Rh,P) being in the range 180−202 Hz and ^2J(Pa,Pb) near 45 Hz. Although two different sulfur substituents exist in complex **2d**, only one doublet resonance due to Rh−P coupling is observed in the $^{31}P\{^1H\}$ NMR at room temperature. The variable-temperature $^{31}P\{^1H\}$ NMR spectra of **2d** in CD_2Cl_2 are displayed in Figure 1. It can be interpreted as an A_2M spin system at room temperature which coalesces at −40 °C. At −90 °C the spectrum features two doublets of doublets corresponding to an ABM spin system. These details are in agreement with the hindered rotation of the $Rh(PPh_3)_2$ moiety about the metal−carborane ligand axis.[2f]

The spectroscopic data and the elemental analysis are consistent with rhodacarborane complexes containing one charge-compensated monoanionic ligand and two triphenylphosphine ligands coordinated to one Rh(I) atom per molecule. To confirm the molecular architecture of these complexes, a single-crystal diffraction study was performed on **2a**. A simplified drawing of the complex unit is depicted in Figure 2, crystallographic

Table 1. Proton Chemical Shift Data for the Substituent on B(10) for Complexes 2a−f

	δ(^{1}H) (area)		
	CH_3	S−CH_2−	−CH_2−
2a	2.33 (6H)		
2b	1.30 (6H)	2.77 (2H) 3.05 (2H)	
2c		2.96 (2H) 3.31 (2H)	1.87 (2H) 2.19 (2H)
2d	0.78 (3H)	3.00 (2H)	
2e	2.36 (3H) 2.73 (3H)		
		2.45 (1H) 2.59 (1H)	
2f	1.05 (3H) 1.61 (3H)		
		2.96 (1H) 3.30 (1H)	

Table 2. $^{31}P\{^1H\}$ Chemical Shifts for Compounds 2a−f

complex	δ(^{31}P)
2a	42.6 (192)[a]
2b	42.5 (192)[a]
2c	43.9 (192)[a]
2d	43.0 (192)[a]
2e	43.1 (202/43)[b]/33.9 (181/43)[b]
2f	42.1 (199/47)[b]/33.3 (182/47)[b]

[a] *J*(P,Rh). [b] *J*(P,Rh)/*J*(P,P)

(8) Tutusaus, O.; Viñas, C.; Núñez, R.; Teixidor, F.; Demonceau, A.; Delfosse, S.; Noels, A. F.; Mata I.; Molins E. *J. Am. Chem. Soc.* **2003**, *125*, 11830.

(9) (a) Tutusaus, O.; Delfosse, S.; Demonceau, A.; Noels, A. F.; Núñez, R.; Viñas, C.; F. Teixidor, F. *Tetrahedron Lett.* **2002**, *43*, 983. (b) Tutusaus, O.; Delfosse, S.; Simal, F.; Demonceau, A.; Noels, A. F.; Núñez, R.; Viñas, C.; Teixidor, F. *Inorg. Chem. Commun.* **2002**, *5*, 941. (c) Tutusaus, O.; Delfosse, S.; Demonceau, A.; Noels, A. F.; Viñas, C.; Teixidor, F. *Tetrahedron Lett.* **2003**, *44/46*, 8421.

(10) Maitlis, P. M. *Chem. Soc. Rev.* **1981**, *10*, 1.

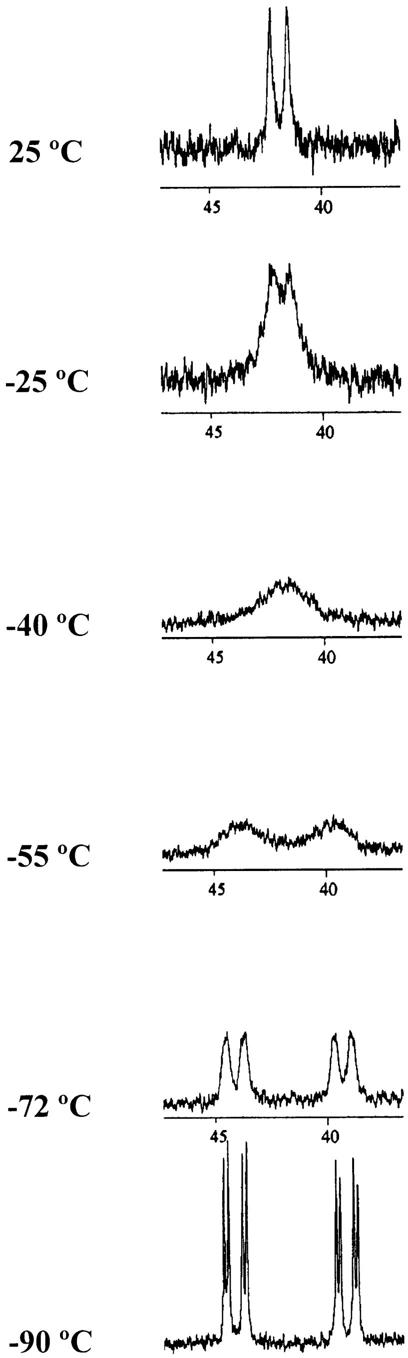

Figure 1. Variable-temperature $^{31}P\{^1H\}$ NMR spectra of complex **2d**.

data are given in Table 3, and selected geometrical parameters are collected in Table 4. Two triphenylphosphine ligands and the boron cage in a η^5 mode coordinate to Rh(I). In the boron cage, C(2), B(4), B(7), and B(8) atoms form short bonds, and the C(1) atom forms a longer bond to Rh(I). A good description of the metal coordination in similar anionic *nido* [C_2B_9] ligands has been published to explain the metal fragment orientation with regard to the cluster.[11] In these reports it was concluded that the metal orientation depends on several factors; the most relevant ones are as follows: the nature of the metal ion,[11b,12] its oxidation state,[3d,11d,13] the nature of the ancillary ligands,[3d] and the cluster substituent and its

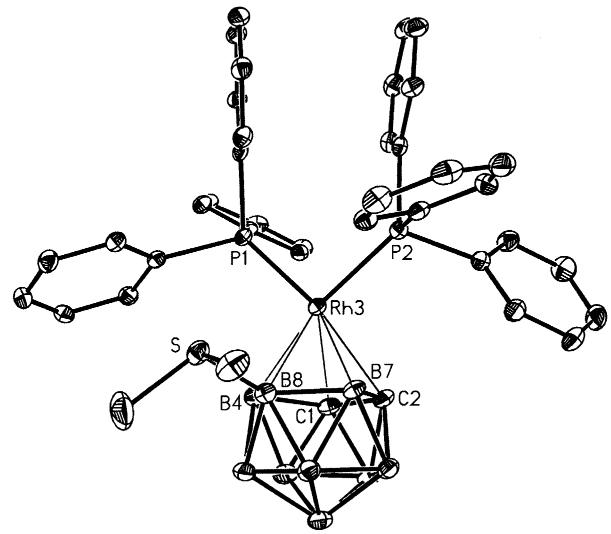

Figure 2. Molecular structure of [3,3-$(PPh_3)_2$-8-SMe_2-*closo*-3,1,2-$RhC_2B_9H_{10}$]·0.912CH_2Cl_2 (**2a**). Hydrogen atoms are omitted for clarity. Displacement ellipsoids are drawn at 30% probability level.

position on the C_2B_3 open face.[14] The reason for the unsymmetrical bonding mode can be that Rh(I) likes to have a square-planar geometry (electronic reason) or there is interaction between the ligands on the coordination sphere. In this case the latter seems to be likely, as in **3** the boron cage bonding is symmetrical (see below). The reason for the asymmetry in **2a** can be result of the interaction of a SMe_2 group with the phenyl groups of the phosphines. The C1−C2 distance is quite short (1.559(6) Å) in **2a**, very close to the cage C−C distance (1.547(4) Å) found in the neutral free 10-(SMe_2)-*nido*-7,8-$C_2B_9H_{11}$ ligand.[6h]

Synthesis and Characterization of [3,3-cod-8-SMe_2-*closo*-3,1,2-$RhC_2B_9H_{10}$]. In a similar way, the reaction of a degassed ethanolic solution of K[10-SMe_2-*nido*-7,8-$C_2B_9H_{10}$] with 0.5 equiv of [RhCl(cod)]$_2$ led to the formation of the yellow compound **3**. All NMR spectra are consistent with a molecule of C_s symmetry. The ^1H NMR spectrum displays resonances at 2.25, 2.43, and 4.37 ppm attributable to the cycloocta-1,5-diene ligand,[3c] and a broad resonance at 3.12 ppm due to the C_c-H protons. The ^{11}B NMR resonances appear in the region between 3.2 and −25.0 ppm, common for *closo* compounds.

Complex **3** crystallized from $CHCl_3$ to give good-quality yellow crystals for X-ray diffraction analysis. The drawing of **3** is shown in Figure 3, and crystallographic data and selected bond parameters are given at Tables 3 and 5, respectively. The molecule consists of a rhodacarborane in a *closo*-icosahedral geometry. In **3** the

(11) (a) Mingos, D. M. P. *J. Chem. Soc., Dalton Trans.* **1977**, 602. (b) Mingos, D. M. P.; Forsyth, M. I.; Welch, A. J. *J. Chem. Soc., Dalton Trans.* **1978**, 1363. (c) Walker, J. A.; Knobler, C. B.; Hawthorne, M. F. *J. Am. Chem. Soc* **1983**, *105*, 3368. (d) Walker, J. A.; Knobler, C. B.; Hawthorne, M. F. *Inorg. Chem.* **1985**, *24*, 2688.

(12) (a) Smith, D. E.; Welch, A. J. *Acta Crystallogr.* **1986**, *C42*, 1717. (b) Colquhoun, H. M.; Greenhough, T. J.; Wallbridge M. G. H. *J. Chem. Soc., Dalton Trans.* **1985**, 761.

(13) Jeffrey, J. C.; Stone Douek, N. L.; Welch, A. J. *J. Chem. Soc., Dalton Trans.* **1993**, 1917.

(14) (a) Baghurst, D. R.; Copley, R. C. B.; Fleischer, H.; Mingos, D. M. P.; Kyd, G. O.; Yellowlees, L. J.; Welch, A. J.; Spalding, T. R.; O'Connell, D. *J. Organomet. Chem.* **1993**, *447*, C14. (b) Robertson, S.; Ellis, D.; Rosair, G. M.; Welch, A. J. *J. Organomet. Chem.* **2003**, *680*, 286.

Table 3. Crystallographic Parameters for 2a·0.912CH_2Cl_2, 3, and 4a·$CHCl_3$

	2a·0.912CH_2Cl_2	**3**	**4a**·$CHCl_3$
empirical formula	$C_{40}H_{46}B_9P_2RhS$·0.912CH_2Cl_2	$C_{12}H_{28}B_9RhS$	$C_{22}H_{31}B_9Cl_2PRhS$·$CHCl_3$
fw	898.25	404.60	748.97
cryst syst	triclinic	monoclinic	monoclinic
cryst habit, color	prism, pale yellow	prism, yellow	plate, red
space group	$P\bar{1}$ (no. 2)	$P2_1/c$	$P2_1$
a (Å)	9.2945(4)	7.086(3)	9.014(2)
b (Å)	12.2403(5)	14.502(9)	18.608(3)
c (Å)	19.7289(7)	18.208(6)	10.060(2)
α (deg)	105.032(3)	90	90
β (deg)	96.062(2)	90.56(3)	100.676(17)
γ (deg)	101.274(2)	90	90
V (Å^3)	2096.72(14)	1871.0(15)	1658.2(6)
Z	2	4	2
T (°C)	−100	20	21
λ	0.71073	0.71069	0.71069
ρ (g cm^{-3})	1.423	1.436	1.500
μ (cm^{-1})	6.81	10.13	10.45
goodness-of-fit[a] on F^2	1.012	1.017	1.082
R^b [$I > 2\sigma(I)$]	0.0468	0.0353	0.0445
$R_w{}^c$ [$I > 2\sigma(I)$]	0.0976	0.0758	0.0947

[a] $S = [\sum w(F_o^2 - F_c^2)^2]/(n - p)^{1/2}$. [b] $R = \sum||F_o| - |F_c||/\sum|F_o|$. [c] $R_w = [\sum w(|F_o^2| - |F_c^2|)^2/\sum w|F_o^2|^2]^{1/2}$.

Table 4. Selected Bond Lengths (Å) and Angles (deg) for 2a·0.912CH_2Cl_2

Rh3−P1	2.2461(10)
Rh3−P2	2.2718(12)
Rh3−C1	2.422(4)
Rh3−C2	2.299(4)
Rh3−B4	2.289(5)
Rh3−B7	2.291(4)
Rh3−B8	2.321(5)
S−B8	1.914(5)
C1−C2	1.559(6)
P1−Rh3−P2	97.13(4)
S−B8−Rh3	108.0(2)
B7−B8−S	122.8(3)
B4−B8−S	123.8(3)

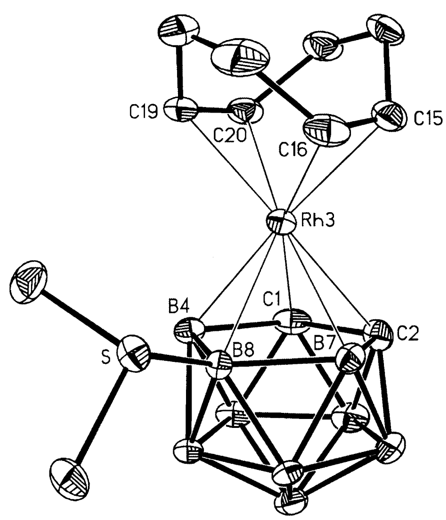

Figure 3. Molecular structure of [3,3-cod-8-SMe_2-*closo*-3,1,2-$RhC_2B_9H_{10}$] (**3**). Hydrogen atoms are omitted for clarity. Displacement ellipsoids are drawn at 20% probability level.

general structural features are similar to those of **2a**, but in **3** a cod molecule has replaced the phosphine ligands of **2a** and the Rh(I) ion is more symmetrically bonded to the boron cage. Moreover, this ligand change results in the boron cage in **3** moving toward Rh(I); in **2a** the distance from the midpoint of the coordinating C_2B_3 pentagon to Rh(I) is 1.812 Å, while in **3** the

Table 5. Selected Bond Lengths (Å) and Angles (deg) for 3

Rh3−C1	2.279(5)
Rh3−C2	2.293(5)
Rh3−C15	2.153(5)
Rh3−C16	2.137(5)
Rh3−C19	2.160(5)
Rh3−C20	2.147(5)
Rh3−B4	2.240(5)
Rh3−B7	2.247(5)
Rh3−B8	2.278(5)
S−B8	1.906(5)
C1−C2	1.559(7)
S−B8−Rh3	112.1(2)
B4−B8−S	126.8(3)
B7−B8−S	120.9(3)

distance is 1.736 Å. Mutual orientations of the SMe_2 groups in **2a** and **3** are different, but the C1−C2 distances are identical [1.559(6) and 1.559(7) Å].

Rh(III) from Rh(I) Metallacarboranes. Dynamic Behavior in Halogenated Solutions. Complexes **2a**−**d** are stable under anaerobic conditions in CH_2Cl_2 and in other nonhalogenated solvents such as toluene, THF, and acetone. In the presence of oxygen, however, total decomposition is observed. Nevertheless, when using halogenated solvents such as $CHCl_3$, CCl_4, $CHBr_3$, or $ClCH_2CH_2Cl$, a change of color from dark yellow to red takes place under N_2, at room temperature, to form the new complexes **4a**−**d**. Contrarily, solutions of **2e**,**f** in the latter solvents are unstable, even under N_2, leading to total decomposition of the product. Compound **3** is stable in all solvents, showing no change.

The spectroscopic data provided some details about the behavior of **2a**−**d** in some halogenated solvents. The $^{31}P\{^1H\}$ NMR spectra showed that the conversion of **2a**−**d** to **4a**−**d** is accompanied by the elimination of PPh_3. In addition, the rate of the reaction depends on the halogenated solvent used, suggesting an active participation of the solvent in the process. Halogenated solvents can be divided depending on the speed of the conversion: (i) the evolution is immediate in halogenated solvents such as CCl_4 and $CHBr_3$, (ii) the reaction is slower, being complete after several hours in $CDCl_3$ or $CHCl_3$, and (iii) no reaction took place in CH_2Cl_2 and halogen-containing aromatic solvents.

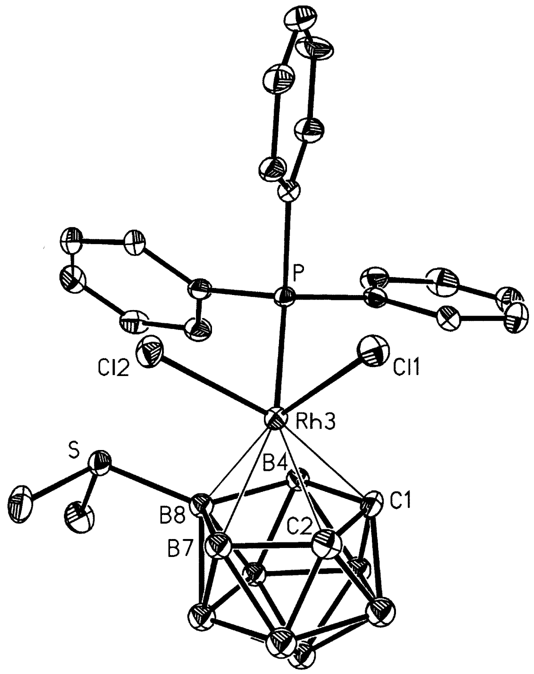

Figure 4. Molecular structure of [3-PPh$_3$-3,3-Cl$_2$-8-SMe$_2$-*closo*-3,1,2-RhC$_2$B$_9$H$_{10}$] (**4a**). Hydrogen atoms are omitted for clarity. Displacement ellipsoids are drawn at 20% probability level.

Table 6. Selected Bond Lengths (Å) and Angles (deg) for 4a·CHCl$_3$

Rh3−Cl1	2.433(3)
Rh3−Cl2	2.386(3)
Rh3−P	2.357(3)
Rh3−C1	2.161(9)
Rh3−C2	2.210(11)
Rh3−B4	2.164(11)
Rh3−B7	2.239(13)
Rh3−B8	2.204(10)
S−B8	1.909(11)
C1−C2	1.649(18)
S−B8−Rh3	114.2(5)
B4−B8−S	126.9(9)
B7−B8−S	121.4(7)

The NMR characterization of compounds **4a**−**d** was originally performed in situ, as products of the conversion of **2a**−**d** in CDCl$_3$. In all cases the ^{11}B{^{1}H} NMR spectra showed a 1:3:2:1:2 pattern and the ^{31}P NMR spectra showed doublets at ca. 25 ppm. These resonances coexist with the presence of PPh$_3$ in the solution.

From a solution of **2a** in CHCl$_3$, red crystals of **4a** precipitated that were good for full characterization by NMR spectroscopy and for single-crystal X-ray diffraction analysis. In the ^{1}H NMR spectrum the cage-carbon hydrogen atoms for **4a** appear at 3.87 ppm, 1.82 ppm shifted to lower field in relation to its precursor **2a**. The ^{11}B{^{1}H} NMR spectrum displays a 1:3:2:1:2 pattern in the range 11 to −14 ppm, thus maintaining the initial *closo* structure of **2a**. A drawing of the complex is shown in Figure 4, crystallographic data are shown in Table 3, and selected geometrical parameters are displayed in Table 6. The structure reveals the formation of [3-PPh$_3$-3,3-Cl$_2$-8-SMe$_2$-*closo*-3,1,2-RhC$_2$B$_9$H$_{10}$], **4a**, a *closo* Rh(III) complex in which the metal exhibits a pseudo-octahedral coordination, with the anionic charge-compensated ligand occupying three facial coordination sites and two chloride ions and a triphenylphosphine ligand occupying the remaining sites. The change from Rh(I) to Rh(III) results in the boron cage becoming even more tightly bonded to the metal ion in **4a** than in **2a** and **3**. The midpoint of the belt in **4a** is 1.618 Å from the Rh(III) cation, and all Rh−B and Rh−C$_c$ bond distances are shorter in **4a** than the relevant distances in **2a** and **3**. As a result of the stronger bonding in **4a,** the C$_2$B$_3$ perimeter is 8.717 Å, while in **2a** it is smaller (8.547 Å). The C1−C2 distance increases to 1.649(18) Å in **4a**, being about 0.09 Å longer than in **2a** and **3**.

Scheme 2. Proposed Mechanism for the Formation of 4a−d from 2a−d in Some Chlorinated Solvents

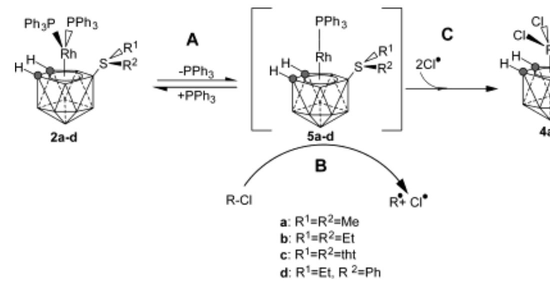

Mechanistic Study. The formation of the new Rh(III) complexes **4a**−**d** from halogenated solutions of the corresponding Rh(I) precursors **2a**−**d** is unprecedented, and no references describing the reaction were found in the literature. It is likely that this transformation requires the loss of a PPh$_3$ ligand in addition to the solvent-assisted oxidation of Rh(I) to Rh(III), which implies coordination of two chlorine atoms.

To elucidate the mechanism of the formation of the Rh(III) complexes from their related Rh(I) species and to understand the nature of the key steps, the transformation of **2a** to **4a** was studied in CDCl$_3$ and CHCl$_3$ using different spectroscopic techniques. First, the importance of the release of the phosphine ligand was evaluated by ^{31}P{^{1}H} NMR by following the progress of a solution of **2a** in CDCl$_3$ containing PPh$_3$ in excess. This slowed the formation of **4a**. On the basis of reactions in which a phosphine dissociative pathway has been well established,[15] we propose that the first step of the reaction involves the dissociation of PPh$_3$, producing an unsaturated 16-electron Rh complex (**5a**), as shown in step A of Scheme 2. In light of these results, the stability of complex **3** in halogenated solvents may be rationalized as a result of the chelating effect of the cod ligand.

Second, the time dependence of the conversion of **2a** to **4a** was monitored in CDCl$_3$ by NMR spectroscopy (Figure 5). The ^{31}P{^{1}H} NMR spectrum of the starting **2a** showed a doublet at 42.6 ppm. As the reaction proceeded, two doublets at 42.6 and 25.9 ppm attributed to **2a** and **4a**, respectively, and a peak assigned to PPh$_3$ were observed. After 90 min, both products are well exhibited. After 3 h, complex **2a** was no longer present and had been transformed into **4a**, as confirmed by the absence of the signal at 42.6 ppm and the presence of

(15) (a) James, B. R.; Markham, L. D. *Inorg. Chem.* **1974**, *13*, 97−100. (b) Hoffman, P. R.; Caulton, K. G. *J. Am. Chem. Soc.* **1975**, *97*, 4221. (c) Bland, W. J.; Davis, R.; Durrant, J. L. *J. Organomet. Chem.* **1984**, *267*, C45−C48. (d) Bland, W. J.; Davis, R.; Durrant, J. L. *J. Organomet. Chem.* **1985**, *280*, 397. (e) Dias, E. L.; Nguyen, S. T.; Grubbs, R. H. *J. Am. Chem. Soc.* **1997**, *119*, 3887. (f) Huang, J.; Stevens, E. D.; Nolan, S. P.; Petersen, J. L. *J. Am. Chem. Soc.* **1999**, *121*, 2674.

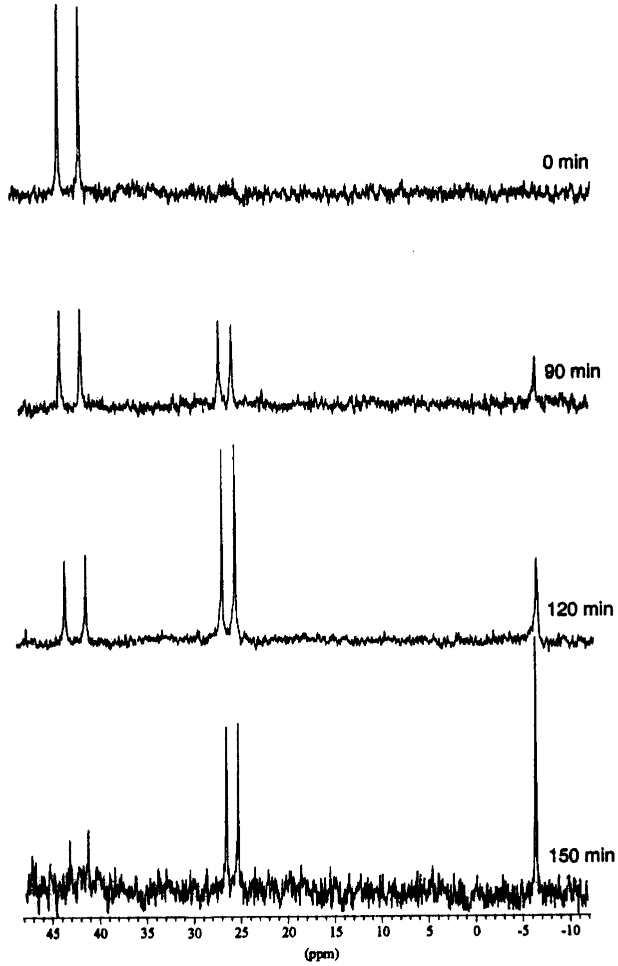

Figure 5. $^{31}P\{^1H\}$ NMR spectra of **2a** in $CDCl_3$ showing the conversion to **4a**.

an intense doublet at 25.9 ppm. The ^1H NMR also supported a mixture of **2a** and **4a** after 30 min, displaying two singlets in the aliphatic region attributed to the SMe_2 protons and two broad resonances at 2.05 and 3.87 ppm, due to the $C_{cluster}$–H protons. The $^{11}B\{^1H\}$ NMR spectrum also showed the formation of new species.

The dynamic study indicates that the release of PPh_3 occurs during the first step (step A, Scheme 2). We suggest that a radical mechanism caused by **5a** occurs, which implies the homolytic cleavage of the halogenated solvent (see step B in Scheme 2). To detect the presence of such free radicals, the EPR spectrum of a $CHCl_3$ solution of **2a** containing an excess of the spin-trap *N-tert*-butyl-α-phenylnitrone (PBN) was recorded. Figure 6 presents the EPR spectrum, as well as the EPRFTSM simulated spectrum,[16] showing a set of three equally spaced doublets centered at $g = 2.0054$ due to the coupling with one N and one H nucleus. The hyperfine splitting constants derived from the fitting procedure are $a_N = 14.6$ G and $a_H = 2.26$ G and are attributable to the PBN-trapped $CHCl_2^{\bullet}$ radical following comparison with literature values.[17] The PBN-trapped $Cl^{\bullet}$ radical is also generated but is not detected at the EPR spectrum due to its very short lifetime. No reddening of the solution was observed in the presence of the spin-trap PBN, which indicates that the PBN had trapped the $Cl^{\bullet}$ radicals, preventing the oxidation of **5a**. Consequently, the cleavage of the solvent was conducted by **5a** (step B, Scheme 2) prior to its oxidation to **4a**; later on, in a reaction in which PBN had not been added, **5a** would capture the $Cl^{\bullet}$ radicals to yield **4a** (step C, Scheme 2). This analysis clearly evidences the formation of free radicals as intermediates in the evolution of **2a** to **4a**.

No such behavior has been mentioned in the previously reported and structurally analogous Rh(I) complexes with isomeric charge-compensated ligands. Examples included [3,3-$(PPh_3)_2$-4-C_5H_5N-*closo*-3,1,2-$RhC_2B_9H_{10}$], [3-PPh_3-3-CO-4-C_5H_5N-*closo*-3,1,2-$RhC_2B_9H_{10}$],[2e,f] [3,3-$(CO)_2$-4-SMe_2-*closo*-3,1,2-$RhC_2B_9H_{10}$], and [1-Ph-3,3-$(CO)_2$-7-SMe_2-*closo*-3,1,2-$RhC_2B_9H_{10}$].[3d,e] The

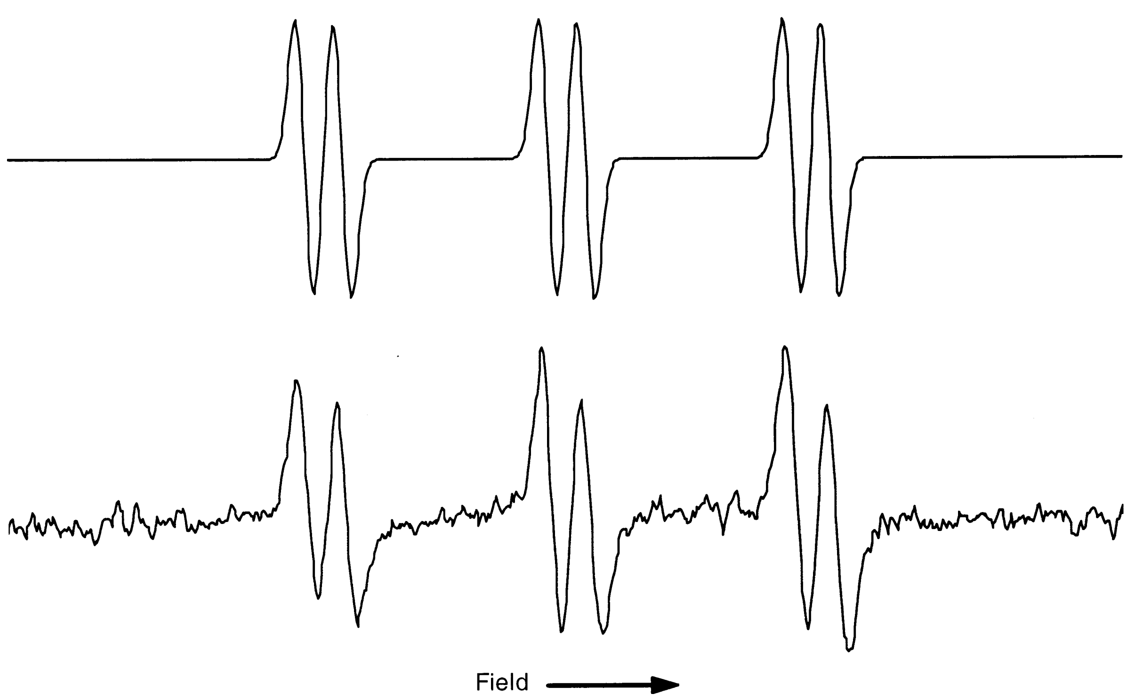

Figure 6. Simulated and experimental EPR spectrum of PBN adducts observed in a $CHCl_3$ solution of **2a**.

only reported example in which oxidation was accomplished was by direct reaction of [3,3-$(CO)_2$-4-SMe_2-*closo*-3,1,2-$RhC_2B_9H_{10}$] with iodine in ether to afford [3-(CO)-3,3-$(I)_2$-4-SMe_2-*closo*-3,1,2-$RhC_2B_9H_{10}$].[3h]

Conclusions

In view of the results, we can deduce that Rh(I) complexes containing the charge-compensated cluster [10-L-*nido*-7,8-$C_2B_9H_{10}$]$^-$ and PPh_3 as ancillary ligands may be easily oxidized to Rh(III) complexes under N_2 atmosphere in some halogenated solvents. The donor capacity of the B(10)-substituted cluster,[8] facilitated by the presence of labile ligands in the molecule, may be the key to causing the process. The capacity to stabilize both Rh(I) and Rh(III) oxidation states by the same system may be attributed to the to-and-fro electron density movement, facilitated by the uniqueness of the boron cluster−sulfonium bridge.[8] This property could be essential in some catalytic processes, which leads to thinking that the rhodium systems will be active as catalysts. The determination of the catalytic activity of these compounds is underway.

Experimental Section

Instrumentation. Microanalyses were performed in our analytical laboratory using a Carlo Erba EA1108 microanalyzer. IR spectra were recorded with KBr pellets on a Shimadzu FTIR-8300 spectrophotometer. The ^{1}H (300.13 MHz), ^{11}B, ^{11}B{^{1}H} (96.29 MHz), and ^{31}P{^{1}H } NMR (121.5 MHz) spectra were recorded on a Bruker ARX 300 instrument equipped with the appropriate decoupling accessories at room temperature. All NMR measurements were performed in deuterated solvents at 22 °C. Chemical shift data for ^{1}H and ^{13}C {^{1}H} NMR spectra were referenced to $SiMe_4$, those for ^{11}B-{^{1}H} and ^{11}B NMR spectra were referenced to external BF_3·Et_2O, and those for ^{31}P{^{1}H} NMR spectra were referenced to external 85% H_3PO_4 (minus values upfield). Chemical shifts were reported in ppm, followed by a description of the multiplet (e.g., d = doublet) and its relative intensity, and all coupling constants are reported in hertz. EPR spectra at room temperature were run with an X-Band Bruker ESP 300E spectrometer equipped with a rectangular cavity operating in a T102 mode, a field frequency lock ER 033M system, and an NMR gaussmeter ER035M.

Materials. All manipulations were carried out under a dinitrogen atmosphere using standard Schlenk techniques. Solvents were purified by distillation from appropriate drying agents before use. Deuterated solvents for NMR (Fluorochem) were freeze−pump−thawed three times under N_2 and transferred to the NMR tube using standard vacuum line techniques. **1a**−**c**[6e] were synthesized as described in the literature. **1d**−**f**[6h] were also freshly prepared. [RhCl$(PPh_3)_3$] and [RhCl(cod)]$_2$ were synthesized according to the literature.[18] All organic and inorganic salts were Fluka or Aldrich analytical reagent grade and were used as purchased. The solvents were reagent grade.

Preparation of [3,3-$(PPh_3)_2$-8-SMe_2-*closo*-3,1,2-$RhC_2B_9H_{10}$] (2a). To a deoxygenated solution of ethanol (15 mL) containing carborane zwitterion **1a** (110 mg, 0.565 mmol) and K[*t*-BuO] (67 mg, 0.597 mmol) was added [RhCl$(PPh_3)_3$] (522 mg, 0.564 mmol), and the mixture was stirred for 3 h at room temperature. Within 1 h the color of the mixture changed from red-brown, characteristic of Wilkinson's catalyst, to pale brown-yellow. After this time, the solid was filtered off and washed with two 15 mL portions of water, 15 mL of ethanol, and two 15 mL portions of diethyl ether. Finally, the solid was dried in vacuo. Compound **2a** was obtained as an amorphous solid. Yield: 364 mg, 79%. ^{1}H NMR ($CDCl_3$): δ 2.05 (br s, 2H, C_c−*H*), 2.33 (s, 6H, S−CH_3), 6.90−7.92 (m, 30H, C_6H_5). ^{31}P-{^{1}H} NMR ($CDCl_3$): δ 42.6 (d, ^1J(P,Rh) = 192). ^{11}B NMR ($CDCl_3$): δ 1.3 (s, 1B), −16.8 (d, ^1J(B,H) = 129, 4B), −22.1 (4B). FTIR (KBr), ν (cm^{-1}): 2545 (B−H). Anal. Calcd for $C_{40}H_{46}B_9P_2RhS$: C, 58.52; H, 5.65; S, 3.91. Found: C, 58.49; H, 5.77; S, 3.79.

Preparation of [3,3-$(PPh_3)_2$-8-SEt_2-*closo*-3,1,2-$RhC_2B_9H_{10}$] (2b). The process was the same as for compound **2a** using 130 mg (0.584 mmol) of **1b**, 69 mg (0.615 mmol) of K[*t*-BuO], and 537 mg (0.580 mmol) of [RhCl$(PPh_3)_3$] in 15 mL of deoxygenated ethanol. The mixture was stirred for 3 h at room temperature, obtaining a pale brown-yellow solid. The solid was filtered and washed as described above to give **2b** (yield: 376 mg, 76%). ^{1}H NMR ($CDCl_3$): δ 1.30 (t, 6H, *J*(H,H) = 7.4, CH_3), 2.10 (br s, 2H, C_c−*H*), 2.77 (m, 2H, S−CH_2), 3.05 (m, 2H, S−CH_2), 7.08−7.54 (m, 30H, C_6H_5). ^{31}P{^{1}H} NMR ($CDCl_3$): δ 42.5 (d, ^1J(P,Rh) = 192). ^{11}B NMR ($CDCl_3$): δ 1.8 (s, 1B), −16.6 (d, ^1J(B,H) = 126, 4B), −22.4 (4B). FTIR (KBr), ν (cm^{-1}): 2535 (B−H). Anal. Calcd for $C_{42}H_{50}B_9P_2RhS$: C, 59.41; H, 5.94; S, 3.78. Found: C, 58.55; H, 5.72; S, 3.68.

Preparation of [3,3-$(PPh_3)_2$-8-$S(CH_2)_4$-*closo*-3,1,2-$RhC_2B_9H_{10}$] (2c). The process was the same as for compound **2a** using 125 mg (0.566 mmol) of **1c**, 67 mg (0.597 mmol) of K[*t*-BuO], and 552 mg (0.564 mmol) of [RhCl$(PPh_3)_3$] in 15 mL of deoxygenated ethanol. The mixture was stirred for 3 h at room temperature, obtaining a pale brown-yellow solid. The solid was filtered and washed as described above to give **2c** (yield: 412 mg, 86%). ^{1}H NMR ($CDCl_3$): δ 1.87 (m, 2H, CH_2), 2.03 (br s, 2H, C_c−*H*), 2.19 (m, 2H, CH_2), 2.96 (m, 2H, S−CH_2), 3.31 (m, 2H, S−CH_2), 7.10−7.65 (m, 30H, C_6H_5). ^{31}P{^{1}H} NMR ($CDCl_3$): δ 43.9 (d, ^1J(P,Rh) = 192). ^{11}B NMR ($CDCl_3$): δ 1.1 (1B), −16.8 (d, ^1J(B,H) = 119, 4B), −21.7 (2B), −23.9 (2B). FTIR (KBr), ν (cm^{-1}): 2541 (B−H). Anal. Calcd for $C_{42}H_{48}B_9P_2RhS$: C, 59.55; H, 5.71; S, 3.79. Found: C, 58.85; H, 5.65; S, 3.67.

Preparation of [3,3-$(PPh_3)_2$-8-SEtPh-*closo*-3,1,2-$RhC_2B_9H_{10}$] (2d). The process was the same as for compound **2a** using 125 mg (0.461 mmol) of **1d**, 54 mg (0.481 mmol) of *t*-BuOK, and 425 mg (0.459 mmol) of [RhCl$(PPh_3)_3$] in 15 mL of deoxygenated ethanol. The mixture was stirred for 3 h at room temperature, obtaining a pale brown-yellow solid. The solid was filtered and washed to give **2d** (yield: 311 mg, 76%). ^{1}H NMR ($CDCl_3$): δ 0.78 (t, 3H, *J*(H,H) = 7.4, CH_3), 2.93 (br s, 2H, C_c−*H*), 3.00 (q, 2H, *J*(H,H) = 7.4, S−CH_2), 6.99−7.57 (m, 35H, C_6H_5). ^{31}P{^{1}H} NMR ($CDCl_3$): δ 43.0 (d, ^1J(P,Rh) = 192). ^{11}B NMR ($CDCl_3$): δ 0.6 (1B), −11.9 (d, ^1J(B,H) = 118, 1B), −16.5 (2B), −21.9 (d, ^1J(B,H) = 109, 5B). FTIR (KBr), ν (cm^{-1}): 2565, 2533, 2513 (B−H). Anal. Calcd for $C_{46}H_{49}B_9P_2RhS$: C, 61.66; H, 5.51; S, 3.58. Found: C, 61.67; H, 5.51; S, 3.65.

Preparation of [1-Me-3,3-$(PPh_3)_2$-8-SMe_2-*closo*-3,1,2-$RhC_2B_9H_9$] (2e). The process was the same as for compound **2a** using 125 mg (0.599 mmol) of **1e**, 70 mg (0.623 mmol) of K[*t*-BuO], and 551 mg (0.595 mmol) of [RhCl$(PPh_3)_3$] in 15 mL of deoxygenated ethanol. The mixture was stirred for 3 h at room temperature, obtaining a pale brown-yellow solid. The solid was filtered and washed as described above to give **2e** (yield: 388 mg, 78%). ^{1}H NMR ($CDCl_3$): δ 1.95 (s, 3H, C_c−CH_3), 2.36 (s, 3H, S−CH_3), 2.73 (s, 3H, S−CH_3), 7.10−7.53 (m, 30H, C_6H_5). ^{31}P{^{1}H} NMR ($CDCl_3$): δ 43.1 (dd, ^1J(P,Rh) = 202, ^2J(P,P) = 43), 33.9 (dd, ^1J(P,Rh) = 181, ^2J(P,P) = 43). ^{11}B NMR ($CDCl_3$): δ 1.7 (s, 1B), −12.2 (d, ^1J(B,H) = 130, 1B), −15.0 (1B), −17.2 (d, ^1J(B,H) = 143, 2B), −19.3 (1B), −21.0 (d, ^1J(B,H) = 122, 2B), −24.3 (1B). FTIR (KBr), ν (cm^{-1}): 2516, 2550 (B−H). Anal. Calcd for $C_{41}H_{48}B_9P_2RhS$: C, 58.97; H, 5.79; S, 3.84. Found: C, 58.26; H, 5.56; S, 3.71.

(16) Kirste, B. *EPRFTSM Program*; Freie Universität Berlin, 1991.
(17) Buettner, G. R. *Free Radical Biol. Med.* **1987**, *3*, 259.
(18) (a) Osborn, J. A.; Wilkinson, G. *Inorg. Synth.* **1966**, *8*, 214. (b) Osborn, J. A.; Wilkinson, G. *Inorg. Synth.* **1967**, *10*, 67.

Preparation of [1-Me-3,3-$(PPh_3)_2$-8-SEt_2-*closo*-3,1,2-$RhC_2B_9H_9$] (2f). The process was the same as for compound **2a** using 113 mg (0.477 mmol) of **1f**, 56 mg (0.499 mmol) of K[*t*-BuO], and 440 mg (0.475 mmol) of $[RhCl(PPh_3)_3]$ in 15 mL of deoxygenated ethanol. The mixture was stirred for 3 h at room temperature, obtaining a brown-yellow solid. The solid was filtered and washed to give **2f** (yield: 280 mg, 68%). ^{1}H NMR (CD_2Cl_2): δ 1.05 (t, 3H, $J(H,H) = 7.3$, CH_3), 1.61 (t, 3H, $J(H,H) = 7.3$, CH_3), 1.29 (br s, 1H, C_c−*H*), 1.69 (s, 3H, CH_3), 2.45 (m, 1H, SCH_2), 2.59 (m, 1H, SCH_2), 2.96 (m, 1H, SCH_2), 3.30 (m, 1H, SCH_2), 7.05−7.90 (m, 30H, C_6H_5). ^{31}P{^{1}H} NMR (CD_2Cl_2): δ 42.1 (dd, ^1J(P,Rh) = 199; ^2J(P,P) = 47), 33.3 (dd, ^1J(P,Rh) = 182; ^2J(P,P) = 47). ^{11}B NMR (CD_2Cl_2): δ 1.0 (s, 1B), −16.3 (d, ^1J(B,H) = 134, 2B), −17.8 (1B), −19.9 (1B), −22.1 (d, ^1J(B,H) = 140, 2B), −23.5 (1B), −26.3 (1B). FTIR (KBr), ν (cm^{-1}): 2519, 2551, 2573 (B−H). Anal. Calcd for $C_{43}H_{52}B_9SP_2Rh$: C, 59.84; H, 6.07; S, 3.71. Found: C, 59.36; H, 5.87; S, 3.22.

Preparation of [3,3-(cod)-8-SMe_2-*closo*-3,1,2-$RhC_2B_9H_{10}$] (3). To a deoxygenated solution of ethanol (15 mL) containing carborane zwitterion **1a** (100 mg, 0.515 mmol) and K[*t*-BuO] (64 mg, 0.540 mmol) was added $[RhCl(cod)]_2$ (124 mg, 0.256 mmol), and the mixture was stirred for 2 h at room temperature. After this time, a bright yellow solid was formed, which was filtered and washed with 10 mL of ethanol. Finally, the solid was dried in vacuo. Compound **3** was obtained as a bright yellow solid. Yield: 110 mg, 53%. ^{1}H NMR ($CDCl_3$): δ 2.25 (m, 4H, CH_2), 2.43 (m, 4H, CH_2), 2.63 (s, 6H, S−CH_3), 3.12 (br s, 2H, C_c−*H*), 4.37 (m, 4H, CH_2). ^{11}B NMR ($CDCl_3$): δ 3.2 (1B), −14.4 (d, ^1J(B,H) = 143, 3B), −16.4 (d, ^1J(B,H) = 181, 2B) −22.1 (d, ^1J(B,H) = 155, 2B), −24.9 (d, ^1J(B,H) = 166, 1B).^{13}C{^{1}H} NMR ($CDCl_3$): δ 26.4, 32.3, 38.4, 75.6 (d, J(C_c,-Rh) = 13). FTIR (KBr), ν (cm^{-1}): 2543, 2504, 2679 (B−H). Anal. Calcd for $C_{12}H_{28}B_9RhS$: C, 35.62; H, 6.98; S, 7.93. Found: C, 35.39; H, 6.78; S, 7.69.

Preparation of [3-PPh_3-3,3-Cl_2-8-SMe_2-*closo*-3,1,2-$RhC_2B_9H_{10}$] (4a). When compound **2a** was dissolved in CHX_3, the color of the solution changed from the initial pale brown-yellow to red. When X = Br, I, the reaction occurred immediately, but when X = Cl, it took 3 h. Red crystals of **4a** were obtained after leaving the solution for 2 days in $CHCl_3$ (85%). ^{1}H NMR ($(CD_3)_2CO$): δ 2.28 (s, 6H, S−CH_3), 3.87 (br s, 2H, C_c−*H*), 7.35−8.02 (m, 15H, C_6H_5). ^{31}P{^{1}H} NMR ($(CD_3)_2CO$): δ 25.9 (d, ^1J(P,Rh) = 124). ^{11}B NMR ($(CD_3)_2CO$): δ 10.8 (d, ^1J(B,H) = 141, 1B), 5.7 (3B), −3.2 (d, ^1J(B,H) = 139, 2B), −10.8 (1B), −14.2 (d, ^1J(B,H) = 159, 2B). ^{13}C{^{1}H} NMR ($(CD_3)_2CO$: δ 26.5, 128.4, 130.5, 132.0, 133.6, 134.9. FTIR (KBr), ν (cm^{-1}): 2553 (B−H). Anal. Calcd for $C_{22}H_{31}B_9Cl_2PRhS{\cdot}0.7CHCl_3$: C, 38.32; H, 4.63; S, 4.13. Found: C, 38.23; H, 4.45; S, 4.49.

Preparation of [3-PPh_3-3,3-Cl_2-8-SEt_2-*closo*-3,1,2-$RhC_2B_9H_{10}$)] (4b). Complex **4b** was formed from a solution of compound **2b** in 5 mL of $CDCl_3$. The formation of this complex was only monitored by NMR in solution, but **4b** was not isolated. ^{1}H NMR ($CDCl_3$): δ 1.12 (t, 6H, CH_3), 2.46 (m, 2H, S−CH_2), 3.04 (m, 2H, S−CH_2), 3.85 (br s, 2H, C_c−*H*), 7.35−8.02 (m, 15H, C_6H_5). ^{31}P{^{1}H} NMR ($CDCl_3$): δ 25.1 (d, ^1J(P,Rh) = 121). ^{11}B NMR ($CDCl_3$): δ 6.4 (d, ^1J(B,H) = 125, 1B), 0.4 (3B), −8.5 (d, ^1J(B,H) = 128, 2B), −15.5 (1B), −19.3 (d, ^1J(B,H) = 143, 2B). ^{13}C{^{1}H} NMR: δ 12.2, 36.5, 128.4, 130.5, 132.0, 133.8.

Preparation of [3-PPh_3-3,3-Cl_2-8- $S(CH_2)_4$-*closo*-3,1,2-$RhC_2B_9H_{10}$)] (4c). The procedure was the same as for compound **4b** using compound **2c** in 5 mL of $CDCl_3$. ^{1}H NMR ($CDCl_3$): δ 1.28 (m, 2H, CH_2), 1.99 (m, 2H, CH_2), 2.85 (m, 2H, S−CH_2), 3.01 (m, 2H, S−CH_2), 3.87 (br s, 2H, C_c−*H*), 7.37−8.07 (m, 15H, C_6H_5). ^{31}P{^{1}H} NMR ($CDCl_3$): δ 25.5 (d, ^1J(P,Rh) = 121). ^{11}B NMR ($CDCl_3$): δ 6.3 (d, ^1J(B,H) = 125, 1B), 1.6 (1B), −0.3 (2B), −8.3 (d, ^1J(B,H) = 128, 2B), −15−3 (1B), −19.2 (2B).

Preparation of [3-PPh_3-3,3-Cl_2-8-SEtPh-*closo*-3,1,2-$RhC_2B_9H_{10}$)] (4d). The process was the same as for compound **4b** using compound **2d** in 5 mL of $CDCl_3$. ^{1}H NMR ($CDCl_3$): δ 1.13 (t, 3H, CH_3), 2.83 (br s, 1H, C_c−*H*), 3.24 (m, 1H, S−CH_2), 3.22 (m, 1H, S−CH_2), 4.57 (br s, 1H, C_c−*H*), 7.08−8.02 (m, 20H, C_6H_5). ^{31}P{^{1}H} NMR ($CDCl_3$): δ 24.8 (d, ^1J(P,Rh) = 118). ^{13}C{^{1}H} NMR: δ 12.2, 36.5, 128.4, 130.5, 132.0, 133.8. ^{11}B NMR ($CDCl_3$): δ 5.6 (1B), 0.8 (1B) −1.7 (2B), −5.9 (2B), −15.3 (d, ^1J(B,H) = 123, 1B), −18.4 (2B).

Kinetic Experiments. A weighed amount of **2a** was placed in a small container, 0.5 mL of $CDCl_3$ was added, and the time counter was reset. The mixture was stirred until dissolution, and the solution was transferred to a NMR tube. The NMR spectrometer was configured to obtain the ^{1}H{^{11}B}, ^{31}P{^{1}H}, and ^{11}B{^{1}H} NMR spectra at preselected time intervals. After the experiment was finished the spectra were integrated and the percent composition of the mixture was calculated.

X-ray Structure Determinations of 2a·0.912CH_2Cl_2, 3, and 4a·$CHCl_3$. Single-crystal data collection for **2a**·0.912CH_2Cl_2 was performed at −100 °C with an Enraf Nonius KappaCCD diffractometer, while the collections for **3** and **4a**·$CHCl_3$ were performed at ambient temperature with a Rigaku AFC5S diffractometer using graphite-monochromatized Mo Kα radiation. A total of 7347, 3306, and 3026 unique reflections were collected for **2a**·0.912CH_2Cl_2, **3**, and **4a**·$CHCl_3$, respectively.

The structures were solved by direct methods and refined on F^2 by the SHELXL97 program.[19] For **2a**·0.912CH_2Cl_2 and **3**, all non-hydrogen atoms were refined with anisotropic displacement parameters. For **4a**·$CHCl_3$, boron atoms were refined with isotropic but the rest of the non-hydrogen atoms with anisotropic displacement parameters. For all structures, the hydrogen atoms were treated as riding atoms using the SHELX97 default parameters. **4a**·$CHCl_3$ crystallizes in a noncentrosymmetric space group, and the absolute configuration of **4a**·$CHCl_3$ was determined by refinement of the Flack *x* parameter. Crystallographic parameters for **2a**·0.912CH_2Cl_2, **3**, and **4a**·$CHCl_3$ are gathered in Table 3.

Acknowledgment. We thank MCyT (project MAT01-1575) and Generalitat de Catalunya 2001/SGR/00337 for partial support of this research. O.T. thanks Ministerio de Educación, Cultura y Deporte for a grant (PN98 43734817).

Supporting Information Available: Tables listing detailed crystallographic data, atomic positional and thermal displacement parameters, and bond lengths and angles for [3,3-$(PPh_3)_2$-8-SMe_2-*closo*-3,1,2-$RhC_2B_9H_{10}$]·0.912CH_2Cl_2 (**2a**·0.912CH_2Cl_2), [3,3-cod-8-SMe_2-*closo*-3,1,2-$RhC_2B_9H_{10}$]·(**3**), and [3-PPh_3-3,3-Cl_2-8-SMe_2-*closo*-3,1,2-$RhC_2B_9H_{10}$]·$CHCl_3$ (**4a**·$CHCl_3$). This material is available free of charge via the Internet at http://pubs.acs.org.

OM030635H

(19) Sheldrick, G. M. *SHELX97*; University of Göttingen: Germany, 1997.